Arch. Mech., **54**, 5-6, pp. 389–410, Warszawa 2002

A new integration procedure for thermo-elasto-viscoplasticity

W. DORNOWSKI

Institute of Fundamental Technological Research,
Polish Academy of Sciences,
Świętokrzyska 21, 00-049 Warsaw, Poland
e-mail: wdorn@ippt.gov.pl

Dedicated to Professor Piotr Perzyna
on the occasion of his 70^{th} birthday

A NUMERICAL INTEGRATION algorithm for thermo-elasto-viscoplastic constitutive equations is presented. This algorithm satisfies the principle of material objectivity with respect to the total motion (translation, rotation and strain) of a material element. For this purpose, the properties of convective description are used. The explicit-implicit integration scheme for the plastic flow rule plays the crucial role in the proposed algorithm. The method of determining the stress state for inelastic deformations is based on the iterative solution of the dynamic yield condition with respect to the norm of the viscoplastic deformation rate tensor. The constitutive model being the subject of numerical analyses is described. Results of numerical calculations, which show an excellent performance of the proposed procedure, are presented.

1. Introduction

CONTEMPORARY DEVELOPMENT of computer technologies gives hope that a more realistic numerical simulation of deformation and fracture processes for metal structures will be possible in the near future. The effective execution of such a simulation demands an analysis of detailed problems connected with the theoretical investigation and experimental identification of constitutive models for structural materials. The applied numerical method as well as the spatial modelling of structures and their loads must be carefully considered too.

The main objective of the paper is to formulate a numerical integration algorithm for thermo-elasto-viscoplastic constitutive relations. In this formulation, the material objectivity in relation to the total motion (translation, rotation and deformation) of a structural element is postulated. The proposed algorithm can be used for the numerical analysis of large deformations and fracture of metal structural elements under monotonic or cyclic loadings.

Numerical integration procedures for elasto-viscoplastic constitutive relations, applied in the finite element or finite difference methods, are based on

the additive structure of these relations. In these procedures, two fundamental parts may be distinguished. In the first part, the so-called elastic trial state, represented by a point of the stress space, is determined. If this point lies beyond the elastic region determined by the yield surface, this means that the plastic flow process is achieved locally. Thus, the principal problem of the second part is to determine the stress state represented by a point of the actual yield surface.

The numerical integration algorithms for elasto-viscoplastic or elasto-plastic constitutive relations, which exist in the literature, differ in manners of determining the stress state for the inelastic deformation. In the procedure for plastically incompressible materials (J_2 flow theory), originally proposed in [33], the flow stresses are determined by the orthogonal projection of trial stresses onto the yield surface. Generalisations of this algorithm for plastic materials with linear isotropic and kinematic hardening have been proposed in [17, 18, 27].

Other generalisations have been referred to a wider class of materials described by non-associative plastic flow rules, arbitrary yield criteria and more complicated hardening laws. In addition, a general elastic response is considered, not restricted to constant elasticities. In such cases, the path of stress projection is already not represented by the straight line in the stress space and it has to be determined numerically. Algorithms of this type are based on the so-called return mapping method [3, 22, 31, 32]. In this method, as a result of integration of elastic equations, the elastic prediction is obtained to determine the initial conditions for plastic equations. Relaxation relations for both stresses and internal state variables define the plastic correction, which is necessary to assure the plastic consistency. The numerical relaxation process is carried out in a step-by-step fashion. At each iteration the yield function is linearized around the current values of state variables. The linearized yield function is represented by a plane contained in the stress space. In order to determine the next iteration the stresses are projected onto this plane. In the limit, such a plane becomes tangent to the yield surface and plastic consistency is restored.

From the computational standpoint, the central issue to be addressed concerns the numerical integration of the constitutive model in such a manner that the resulting discrete equations identically satisfy the principle of material frame indifference. Satisfaction of this fundamental restriction leads to the so-called incrementally objective algorithms [15, 26, 29]. The material objectivity for the superimposed spatial rigid body motion has been considered most often.

Constitutive equations, which are assumed to be the object of the numerical analysis, are presented in Sec. 2. Within the framework of the rate-type covariance, material structure with a finite set of the internal state variables, the viscoplastic effects, plastic strain induced anisotropy (kinematic hardening), micro-damage mechanisms, isotropic hardening, plastic spin effects as well as thermomechanical couplings are taken into account.

The proposed numerical integration algorithm for the given constitutive equations is presented in Sec. 3. Properties of the convective description are used. In the convective coordinate system the rates of spatial tensor fields, objective with respect to the arbitrary spatial diffeomorphism (regular motion), are represented by matrices of partial time derivatives of suitable components of these fields [5]. This property directly leads to the incremental expressions, which are objective in the above sense. The explicit-implicit integration scheme for the plastic flow rule is the essential part of the proposed algorithm. The method of determination of the flow stresses is based on the iterative solution of the dynamic yield condition with respect to the norm of the viscoplastic deformation rate tensor.

A numerical example is presented in Sec. 4. In this example, the capability of the discussed algorithm is shown. A thin steel plate with a narrow notch performed perpendicularly to its edge is analysed numerically by means of the finite difference method. The dynamic cyclic load is assumed. The so-called low-cycle fatigue regime is considered. The evolution of greatest stress regions forming in the neighbourhood of the initial notch is analysed. The numerical simulation of evolutions of plastic zones, temperature, microdamage and plastic rotation in vicinity of the developing fatigue crack is carried out. The adiabatic process is considered.

Final comments and conclusions are presented in Sec. 5.

2. Constitutive foundations

Most of metals show simultaneously plastic and viscous effects. Viscous effects appear most clearly in fast changing processes, but they also influence essentially the rheological phenomena. Physical processes lying at the bases of viscoplastic phenomena have a complicated nature and they depend mostly on the movement of dislocations and on changes of distributions of the dislocation density. Besides, temperature of a material influences strongly the movement of dislocations and the changes of their densities, and thus the viscoplastic phenomena. Temperature activates or breaks these processes [24, 25].

In viscoplasticity, unlike in plasticity, the dependence of plastic deformations is postulated not only on the path of loading, but also on the phenomena of the time scale. This means that viscoplastic materials show simultaneously the sensitivity to the path of loading and to the rate of deformation. In this manner, different magnitudes of the plastic deformations will be obtained for different loading paths and for different deformation rates. The fact, that these two different material sensitivities correspond to two different forms of the internal dissipation, should find a reflection in the constitutive modelling.

Except for viscoplasticity, the effects such as micro-damage, plastic strain-induced anisotropy (kinematic hardening), isotropic hardening, the plastic spin

and the thermomechanical couplings are taken into account [10, 11]. The considerations are limited to the fast changing, adiabatic processes. The spatial description is assumed as physically most natural. Such an approach has also a reason, which results from the application of constitutive equations to the description of plastic flow processes in the actual state.

The considered constitutive relations can be written in the following, comfortable for an incremental analysis, form:

Evolution equation for the Kirchhoff stress tensor τ [5, 6, 11, 12]

$$L_{\mathbf{v}}\boldsymbol{\tau} = L^e : \mathbf{d} - L^e : \mathbf{d}^p - L^{th}\dot{\vartheta} - \mathbf{k} - \mathbf{s}. \tag{2.1}$$

In the above equation the tensorial measure of the stress rate is the Lie derivative of the tensor $\boldsymbol{\tau}$. In the mechanics of continuous media, the notion of the Lie derivative is connected with the material objectivity of rates of spatial tensor fields with respect to the diffeomorphism (regular motion) [11, 20]. The total deformation rate tensor $\mathbf{d}$ and the inelastic deformation rate tensor $\mathbf{d}^p$ are measures of strain rates, which are objective in the above sense. By L^e and L^{th} we denote the tensor of elastic moduli (fourth rank tensor) and the thermal expansion tensor (second rank tensor), respectively. The symbol $\dot{\vartheta}$ denotes the rate of temperature.

Expressions

$$\mathbf{k} = \mathbf{d}^p \cdot \boldsymbol{\tau} - \boldsymbol{\tau} \cdot \mathbf{d}^p, \quad \mathbf{s} = \boldsymbol{\omega}^p \cdot \boldsymbol{\tau} - \boldsymbol{\tau} \cdot \boldsymbol{\omega}^p \tag{2.2}$$

describe the covariant effect and the influence of a plastic spin $\boldsymbol{\omega}^p$, respectively [7].

Plastic flow rule

$$\mathbf{d}^p = \bar{\Lambda}(\tilde{\boldsymbol{\tau}}' + A\mathrm{tr}\tilde{\boldsymbol{\tau}}\mathbf{g}). \tag{2.3}$$

The scalar multiplier $\bar{\Lambda}$ is given by the relation

$$\bar{\Lambda} = \frac{1}{T_m}\langle\Phi(\cdot)\rangle\,(2\tilde{J}_2' + 3A^2\tilde{J}_1^2)^{-1/2}, \tag{2.4}$$

where T_m denotes the relaxation time and Φ is the empirical overstress function [23]. The second invariant of a relative stress deviator $\tilde{\boldsymbol{\tau}}' = \boldsymbol{\tau}' - \boldsymbol{\alpha}'$ is denoted by $\tilde{J}_2'$, and $\tilde{J}_1$ denotes the first invariant of the relative stress $\tilde{\boldsymbol{\tau}} = \boldsymbol{\tau} - \boldsymbol{\alpha}$. The back stress tensor $\boldsymbol{\alpha}$ determines the actual position of the yield surface centre in the stress space and it is the measure of kinematic hardening. Thus, the relative stress expresses the difference between the point of loading and the yield surface centre. By $\mathbf{g}$ the metric tensor of the convective coordinate system is denoted.

The magnitude

$$A = 2\left[n_1(\vartheta) + n_2(\vartheta)\xi\right] \tag{2.5}$$

describes the influence of temperature-dependent micro-damage mechanisms on the plastic flow direction. The scalar parameter ξ expresses the volumetric participation of microdamages in the material.

Equation for the plastic spin [2] has the form

$$\omega^p = \bar{\eta}(\boldsymbol{\alpha} \cdot \mathbf{d}^p - \mathbf{d}^p \cdot \boldsymbol{\alpha}). \tag{2.6}$$

The postulated equation describes the dependence of the plastic spin on the plastic strain-induced anisotropy. Therefore, the plastic spin may be of significance in problems of the cyclic plasticity (accumulation of the plastic rotation at cyclic loads).

Evolution equations for internal state variables [6, 8]

$$L_{\mathrm{v}}\boldsymbol{\mu} = \hat{\mathbf{m}} \tag{2.7}$$

The vector of evolution functions $\hat{\mathbf{m}}$ is determined by analyses of the examined physical processes. It is postulated that the internal state vector $\boldsymbol{\mu}$ has the form $\mu = (\xi, \alpha)$. Evolution equation for temperature (adiabatic process) [9, 19] is

$$\dot{\vartheta} = \frac{\bar{\chi}}{\rho c_p}\tau : \mathbf{d}^p + \frac{\bar{\bar{\chi}}}{\rho c_p}\Xi, \tag{2.8}$$

where ρ is the mass density in the actual configuration, c_p denotes the specific heat, Ξ determines the evolution function for internal micro-damage mechanisms (nucleation, growth and coalescence). By $\bar{\chi}$ and $\bar{\bar{\chi}}$ the irreversibility coefficients are denoted.

Making the operation $\mathbf{d}^p : \mathbf{d}^p$, the dynamic yield criterion is obtained as follows

$$\Theta = \left\{\tilde{J}_2' + \left[n_1(\vartheta) + n_2(\vartheta)\xi\right]\tilde{J}_1^2\right\}^{1/2} - \kappa\left[1 + \Phi^{-1}\left(T_m \left\|\mathbf{d}^{\mathrm{p}}\right\|\right)\right] = 0, \tag{2.9}$$

$$\left\|\mathbf{d}^p\right\| = \left(\mathbf{d}^p : \mathbf{d}^p\right)^{1/2},$$

where κ is the isotropic hardening-softening function. A more detailed discussion of the presented constitutive model can be found in the quoted papers, where wide bibliographic references to the considered problems are presented.

3. A numerical integration algorithm

To construct an incrementally objective algorithm the properties of convective description [13, 14, 21] is used. In this description the rate of spatial tensor field, objective with respect to an arbitrary spatial diffeomorphism (regular motion), is represented by the matrix of partial time derivatives of suitable components of such a field. This property directly leads to the incremental expressions, which are objective in the above sense. For example, in the implicit expression the objective increments of strains and stresses have the following convective representations:

$$\underset{(n)}{\mathbf{d}}\,\Delta t \cong \Delta e_{ij}(\underset{(n)}{\mathbf{g}^i} \otimes \underset{(n)}{\mathbf{g}^j}) \;,\quad \underset{(n)}{L_{\mathbf{v}}\boldsymbol{\tau}}\,\Delta t \cong \Delta \boldsymbol{\tau}^{ij}(\underset{(n)}{\mathbf{g}_i} \otimes \underset{(n)}{\mathbf{g}_i}), \tag{3.1}$$

where

$$\Delta e_{ij} = \underset{(n)}{e_{ij}} - \underset{(n-1)}{e_{ij}} \;,\quad \Delta \boldsymbol{\tau}^{ij} = \underset{(n)}{\boldsymbol{\tau}^{ij}} - \underset{(n-1)}{\boldsymbol{\tau}^{ij}} \tag{3.2}$$

are the increments of convective components of the Euler strain tensor and the Kirchhoff stress tensor, respectively. The defined increments refer to the time increment $\Delta t^{n-1,n} = t^n - t^{n-1}$ (for simplification of the notation the index $(n\text{-}1,n)$ is omitted).

For comparison, in the spatial description referred to the fixed, rectangular system of coordinates $\{x^i\}$ with a basis $\{\mathbf{e}_i\}$, $i = 1,2,3$, the suitable stress increment has the following form:

$$\underset{(n)}{L_{\mathbf{v}}\boldsymbol{\tau}}\,\Delta t \cong \left(\Delta \boldsymbol{\tau}^{ij} + \left.\frac{\partial \boldsymbol{\tau}^{ij}}{\partial x^k}\right|_{(n)} \underset{(n)}{v^k}\,\Delta t - \underset{(n)}{\boldsymbol{\tau}^{kj}} \left.\frac{\partial v^i}{\partial x^k}\right|_{(n)} \Delta t - \underset{(n)}{\boldsymbol{\tau}^{ik}} \left.\frac{\partial v^j}{\partial x^k}\right|_{(n)} \Delta t \right) (\mathbf{e}_i \otimes \mathbf{e}_j), \tag{3.3}$$

where v^i are components of the spatial velocity field. The numerical integration procedure based on the increment (3.3) needs additional calculation of the stress and velocity gradients. In the convective approach this troublesome necessity is not performed. As a result, less complicated and thus more efficient algorithm can be obtained.

In the numerical integration algorithm presented below for the specified constitutive equations the convective approach is just used. Incremental relationships determining the elastic trial state $\breve{\boldsymbol{\tau}}$ ($\mathbf{d}^e = \mathbf{d}$), separated into volumetric and deviatoric parts, have the following form:

$$\operatorname{tr}(\underset{(n)}{L_{\mathbf{v}}\breve{\boldsymbol{\tau}}})\Delta t = (2\mu + 3\lambda)\operatorname{tr}\underset{(n)}{\mathbf{d}}\,\Delta t,\quad \underset{(n)}{L_{\mathbf{v}}\breve{\boldsymbol{\tau}}'}\,\Delta t = 2\mu\,\underset{(n)}{\mathbf{d}'}\,\Delta t, \tag{3.4}$$

where

$$\underset{(n)}{\mathrm{tr}}(L_{\mathbf{v}}\overset{\smile}{\boldsymbol{\tau}})\Delta t = \underset{(n)}{\dot{\overset{\smile}{\tau}}^{ij}}\,\underset{(n)}{\Delta t\, g_{ij}} \cong \underset{(n)}{\Delta\overset{\smile}{\tau}^{ij}}\,\underset{(n)}{g_{ij}}\ ,$$

$$\underset{(n)}{\mathrm{L}_{\mathbf{v}}\overset{\smile}{\boldsymbol{\tau}}'}\,\Delta t = \underset{(n)}{\dot{\overset{\smile}{\tau}}'^{ij}}\,\underset{(n)}{\Delta t(\mathbf{g}_i}\otimes\underset{(n)}{\mathbf{g}_j)} \cong \underset{(n)}{\Delta\overset{\smile}{\tau}'^{ij}}\,\underset{(n)}{(\mathbf{g}_i}\otimes\underset{(n)}{\mathbf{g}_j})\ ,$$

$$\underset{(n)}{\mathrm{trd}}\,\Delta t = \underset{(n)}{\dot{e}_{ij}}\,\underset{(n)}{\Delta t\, g^{ij}} \cong \underset{(n)}{\Delta e_{ij}}\,\underset{(n)}{g^{ij}}\ , \tag{3.5}$$

$$\begin{aligned}\underset{(n)}{\mathbf{d}'}\,\Delta t &= \underset{(n)}{d'_{kl}}\,\Delta t(\underset{(n)}{\overset{k}{\mathbf{g}}}\otimes\underset{(n)}{\mathbf{g}^l})\\ &= \underset{(n)}{\dot{e}'_{kl}}\,\underset{(n)}{\Delta t\, g^{ki}}\,\underset{(n)}{g^{lj}}\underset{(n)}{(\mathbf{g}_i}\otimes\underset{(n)}{\mathbf{g}_j}) \cong \underset{(n)}{\Delta\, e'_{kl}}\,\underset{(n)}{g^{ki}}\,\underset{(n)}{g^{lj}}\underset{(n)}{(\mathbf{g}_i}\otimes\underset{(n)}{\mathbf{g}_j})\ .\end{aligned}$$

By μ and λ the Lamé constants are denoted. It is noteworthy that the product $\underset{(n)}{\dot{e}'_{kl}}\,\underset{(n)}{g^{ki}}\,\underset{(n)}{g^{lj}}$ in Eq. $(3.5)_4$ can not be prescribed as $\underset{(n)}{\dot{e}'^{ij}}$, because $\dot{e}'^{ij} = \overbrace{e'_{kl}g^{ki}g^{lj}} = \dot{e}'_{kl}g^{ki}g^{lj} + e'_{kl}\dot{g}^{ki}g^{lj} + e'_{kl}g^{ki}\dot{g}^{lj}$. Besides, convective components $\dot{e}^{ij}$ do not represent the deformation rate tensor $\mathbf{d}$. They represent another objective rate measure of the Euler strain tensor, i.e. $L_{\mathbf{v}}\mathbf{e} = \dot{\mathbf{e}} - \mathbf{e}\cdot\mathbf{l}^T - \mathbf{l}\cdot\mathbf{e} = \dot{e}^{ij}(\mathbf{g}_i\otimes\mathbf{g}_j)$ [5]. Therefore, the incremental equations (3.4) for the elastic trial state are prescribed in the covariant basis of the convective reference frame.

In the proposed algorithm the following matrix notation for suitable tensor representations is used (for the simplification of notation the index (n) is omitted):

$$\begin{gathered}\mathbf{g} = [g_{ij}]_{3\times3},\quad \mathbf{g}^{-1} = [g^{ij}]_{3\times3},\quad \boldsymbol{\tau} = [\tau^{ij}]_{3\times3},\quad \overset{\smile}{\boldsymbol{\tau}} = [\overset{\smile}{\tau}{}^{ij}]_{3\times3},\\ \Delta\boldsymbol{\tau} = [\Delta\tau^{ij}]_{3\times3},\quad \Delta\overset{\smile}{\boldsymbol{\tau}} = [\Delta\overset{\smile}{\tau}{}^{ij}]_{3\times3},\quad \boldsymbol{\alpha} = [\alpha^{ij}]_{3\times3},\quad \mathbf{d}^p = [d^p_{ij}]_{3\times3},\\ \Delta\mathbf{e} = [\Delta e_{ij}]_{3\times3},\quad \Delta\mathbf{e}^p = [\Delta e^p_{ij}]_{3\times3},\\ \boldsymbol{\omega}^p = [\omega^{pij}]_{3\times3},\quad \mathbf{k} = [k^{ij}]_{3\times3},\quad \mathbf{s} = [s^{ij}]_{3\times3}.\end{gathered} \tag{3.6}$$

At last, the incremental equations for the elastic trial state take the matrix form

$$\mathrm{tr}(\Delta\overset{\smile}{\boldsymbol{\tau}}\mathbf{g}) = (2\mu + 3\lambda)\mathrm{tr}(\Delta\mathbf{e}\mathbf{g}^{-1})\quad \Delta\overset{\smile}{\boldsymbol{\tau}}{}' = 2\mu\mathbf{g}^{-1}\Delta\mathbf{e}'\mathbf{g}^{-1}. \tag{3.7}$$

From Eq. (3.7) the increments of trial stresses in a time interval $[t^{n-1}, t^n]$ are determined. According to the following expressions, the trial stresses may be

determined for a time instant t^n:

$$\text{tr}(\breve{\boldsymbol{\tau}}\mathbf{g}) = \text{tr}(\underset{(n-1)}{\breve{\boldsymbol{\tau}}}\,\mathbf{g}) + \text{tr}(\Delta\breve{\boldsymbol{\tau}}\mathbf{g}), \qquad \breve{\boldsymbol{\tau}}' = \underset{(n-1)}{\breve{\boldsymbol{\tau}}'} + \Delta\breve{\boldsymbol{\tau}}'. \tag{3.8}$$

These stresses are used to check the yield condition.

$$\varphi = \hat{\varphi}(\breve{\boldsymbol{\tau}}, \underset{(n-1)}{\mu}, \underset{(n-1)}{\vartheta}, \underset{(n-1)}{\kappa}). \tag{3.9}$$

If $\varphi \leq 0$ the elastic process takes place and

$$\text{tr}(\boldsymbol{\tau}\mathbf{g}) = \text{tr}(\breve{\boldsymbol{\tau}}\mathbf{g}) \;,\; \boldsymbol{\tau}' = \breve{\boldsymbol{\tau}}'. \tag{3.10}$$

Internal state variables, temperature and the hardening-softening function remain unchanged, i.e. $\mu = \underset{(n-1)}{\mu}$, $\vartheta = \underset{(n-1)}{\vartheta}$ and $\kappa = \underset{(n-1)}{\kappa}$.

If $\varphi > 0$ the inelastic process is achieved locally. Then, the suitable relationships of elasto-viscoplasticity should be considered. In order to describe the incremental form of the plastic flow rule (2.3) the following mixed (explicit-implicit) approach is proposed:

$$\text{tr}\mathbf{d}^p\Delta t = 3\Delta\bar{\Lambda}\underset{(n-1)}{A}\,\text{tr}(\boldsymbol{\tau} - \underset{(n-1)}{\boldsymbol{\alpha}}), \quad \mathbf{d}'^p\Delta t = \Delta\bar{\Lambda}(\boldsymbol{\tau}' - \underset{(n-1)}{\boldsymbol{\alpha}'}), \tag{3.11}$$

where

$$\text{tr}\,\mathbf{d}'^p\,\Delta t = \Delta e^p_{ij}\,g^{ij}, \quad \mathbf{d}'^p\,\Delta t = \Delta e'^p_{kl}\,g^{ki}\,g^{lj}(\mathbf{g}_i \otimes \mathbf{g}_j), \quad \Delta\bar{\Lambda} = \bar{\Lambda}\Delta t. \tag{3.12}$$

All magnitudes prescribed at the right-hand side of equations (3.11), except the stresses, are defined for a time instant t^{n-1} at the beginning of the time step. In this sense, the incremental formulas (3.11) are explicit for internal state variables $\underset{(n-1)}{\xi}$ and $\underset{(n-1)}{\alpha}$, and implicit for stresses. In the matrix notation for suitable tensorial representations, the analysed law takes the form

$$\begin{aligned} &\text{tr}(\Delta\mathbf{e}^p\mathbf{g}^{-1}) = 3\Delta\bar{\Lambda}\underset{(n-1)}{A}\,\text{tr}[(\boldsymbol{\tau} - \underset{(n-1)}{\boldsymbol{\alpha}})\mathbf{g}], \\ &\mathbf{g}^{-1}\Delta\mathbf{e}'^p\,\mathbf{g}^{-1} = \Delta\bar{\Lambda}(\boldsymbol{\tau}' - \underset{(n-1)}{\boldsymbol{\alpha}'}). \end{aligned} \tag{3.13}$$

The incremental form of the evolution equation for the Kirchhoff stress tensor (2.1) in the matrix notation is

$$\begin{aligned} \text{tr}(\Delta\boldsymbol{\tau}\mathbf{g}) &= (2\mu + 3\lambda)\text{tr}(\Delta\mathbf{e}\mathbf{g}^{-1}) - (2\mu + 3\lambda)\text{tr}(\Delta\mathbf{e}^p\mathbf{g}^{-1}) \\ &\quad - 3(2\mu + 3\lambda)\theta\,\underset{(n-1)}{\dot{\vartheta}}\,\Delta t - [\text{tr}(\underset{(n-1)}{\mathbf{k}}\,\mathbf{g}) + \text{tr}(\underset{(n-1)}{\mathbf{s}}\,\mathbf{g})]\Delta t, \end{aligned} \tag{3.14}$$

$$\Delta\boldsymbol{\tau}' = 2\mu\mathbf{g}^{-1}\Delta\mathbf{e}'\mathbf{g}^{-1} - 2\mu\mathbf{g}^{-1}\Delta\mathbf{e}'^p\mathbf{g}^{-1} - (\underset{(n-1)}{\mathbf{k}'} + \underset{(n-1)}{\mathbf{s}'})\Delta t.$$

Taking into account the relationships of the elastic trial state (3.7) it can be noticed that the first components at the right-hand sides of equations (3.14) express the increments of trial stresses. Substituting Eq. (3.7) and Eq. (3.13) into Eq. (3.14) gives the following system of algebraic equations:

$$\text{(3.15)}\quad \operatorname{tr}(\boldsymbol{\tau}\mathbf{g}) = \operatorname{tr}(\underset{(n-1)}{\boldsymbol{\alpha}}\,\mathbf{g}) + \frac{1}{1+3(2\mu+3\lambda)\Delta\bar{\Lambda}\,\underset{(n-1)}{A}}\Big\{\operatorname{tr}[(\breve{\boldsymbol{\tau}} - \underset{(n-1)}{\boldsymbol{\alpha}})\mathbf{g}]$$

$$- 3(2\mu+3\lambda)\theta\,\underset{(n-1)}{\dot{\vartheta}}\,\Delta t - [\operatorname{tr}(\underset{(n-1)}{\mathbf{k}}\,\mathbf{g}) + \operatorname{tr}(\underset{(n-1)}{\mathbf{s}}\,\mathbf{g})]\Delta t\Big\},$$

$$\boldsymbol{\tau}' = \underset{(n-1)}{\boldsymbol{\alpha}'} + \frac{1}{1+2\mu\Delta\bar{\Lambda}}\Big[\breve{\boldsymbol{\tau}}' - \underset{(n-1)}{\boldsymbol{\alpha}'} - (\underset{(n-1)}{\mathbf{k}'} + \underset{(n-1)}{\mathbf{s}'})\Delta t\Big].$$

This system will be appointed with respect to the scalar multiplier $\Delta\bar{\Lambda}$ when the dynamic yield condition (2.9) will be taken into account,

$$\text{(3.16)}\qquad \Theta = f(\boldsymbol{\tau}, \underset{(n-1)}{\boldsymbol{\alpha}}, \underset{(n-1)}{\xi}, \underset{(n-1)}{\vartheta}) - \underset{(n-1)}{\kappa}\,[1 + \Phi^{-1}(T_m\,\|\mathbf{d}^p\|)] = 0.$$

Owing to nonlinearity of this condition, $\Delta\bar{\Lambda}$ has to be determined by an iterative method (e.g. Newton's method). In accordance with Eq. (3.16) the norm of the inelastic deformation rate tensor $\mathbf{d}^p$ is updated at each iteration. For this purpose, the incremental form (3.13) of the inelastic flow rule is used. The iterative procedure of determination of the multiplier $\Delta\bar{\Lambda}$ determines the non-linear path of projection of the trial stress onto the actual yield surface.

After the end of the iterative procedure the temperature ϑ at a time instant t^n is calculated,

$$\text{(3.17)}\qquad \vartheta = \underset{(n-1)}{\vartheta} + \Delta\vartheta, \quad \Delta\vartheta = \frac{\bar{\chi}}{\underset{(n-1)}{\rho}\,c_p}\operatorname{tr}(\boldsymbol{\tau}\Delta\mathbf{e}^p) + \frac{\bar{\bar{\chi}}}{\underset{(n-1)}{\rho}\,c_p}\,\underset{(n-1)}{\Xi}\,\Delta t.$$

Next, the following magnitudes are determined: the internal state variables

$$\text{(3.18)}\qquad \boldsymbol{\mu} = \underset{(n-1)}{\boldsymbol{\mu}} + \Delta\boldsymbol{\mu}, \quad \Delta\boldsymbol{\mu} = \hat{\mathbf{m}}(\boldsymbol{\tau}, \underset{(n-1)}{\boldsymbol{\mu}}, \vartheta)\Delta t,$$

the plastic spin

$$\text{(3.19)}\qquad \boldsymbol{\omega}^p = \bar{\eta}(\boldsymbol{\alpha}\mathbf{d}^p\mathbf{g}^{-1} - \mathbf{g}^{-1}\mathbf{d}^p\boldsymbol{\alpha}),$$

and tensors of the covariant and plastic spin effects:

$$\text{(3.20)}\qquad \mathbf{k} = \mathbf{g}^{-1}\mathbf{d}^p\boldsymbol{\tau} - \boldsymbol{\tau}\mathbf{d}^p\mathbf{g}^{-1}, \quad \mathbf{s} = \boldsymbol{\omega}^p\mathbf{g}\boldsymbol{\tau} - \boldsymbol{\tau}\mathbf{g}\boldsymbol{\omega}^p.$$

The proposed approach gives very good results for calculations with a small time step as in the explicit finite element or finite difference methods that operate with small time steps because of the stability condition. Operating with a greater time step becomes quite possible in the implicit, unconditionally stable methods. In such cases, the implicit forms of relationships (3.13) and (3.14) should be considered, i.e. such in which $\underset{(n)}{\boldsymbol{\mu}}$, $\underset{(n)}{\mathbf{k}}$, $\underset{(n)}{\mathbf{s}}$ and $\underset{(n)}{\dot{\vartheta}}$ are determined at the end of a time step. As a result the system of non-linear, algebraic equations is obtained instead of the system of equations (3.15). From the viewpoint of numerical calculations the solution of such a system is much more expensive (time-consuming).

To describe the analysed method in the form of a numerical algorithm it is assumed that the non-linear equation (3.16) is solved by means of the iterative Newton's method.

1. Geometric update

$$\Delta\mathbf{e} = \mathbf{e} - \underset{(n-1)}{\mathbf{e}}.$$

2. Elastic trial state

$$\mathrm{tr}(\Delta\breve{\boldsymbol{\tau}}\mathbf{g}) = (2\mu + 3\lambda)\mathrm{tr}(\Delta\mathbf{e}\mathbf{g}^{-1}), \quad \Delta\breve{\boldsymbol{\tau}}' = 2\mu\mathbf{g}^{-1}\Delta\mathbf{e}'\mathbf{g}^{-1}$$

$$\mathrm{tr}(\breve{\boldsymbol{\tau}}\mathbf{g}) = \mathrm{tr}(\underset{(n-1)}{\breve{\boldsymbol{\tau}}}\,\mathbf{g}) + \mathrm{tr}(\Delta\breve{\boldsymbol{\tau}}\mathbf{g}), \quad \breve{\boldsymbol{\tau}}' = \underset{(n-1)}{\breve{\boldsymbol{\tau}}'} + \Delta\breve{\boldsymbol{\tau}}'.$$

3. Check the yield condition

$$\hat{\varphi}(\breve{\boldsymbol{\tau}}, \underset{(n-1)}{\boldsymbol{\mu}}, \underset{(n-1)}{\vartheta}, \underset{(n-1)}{\kappa}) \leq 0\ ?$$

YES: $\mathrm{tr}(\boldsymbol{\tau}\mathbf{g}) = \mathrm{tr}(\breve{\boldsymbol{\tau}}\mathbf{g})$, $\boldsymbol{\tau}' = \breve{\boldsymbol{\tau}}'$,

$$\boldsymbol{\mu} = \underset{(n-1)}{\boldsymbol{\mu}}, \quad \vartheta = \underset{(n-1)}{\vartheta}, \quad \kappa = \underset{(n-1)}{\kappa} \rightarrow \mathrm{EXIT}$$

NO: $i = 1, \quad \Delta\bar{\Lambda}^{(i-1)} = \Delta\underset{(n-1)}{\bar{\Lambda}}$.

4. Stresses in the inelastic state

$$\mathrm{tr}(\boldsymbol{\tau}^{(i)}\mathbf{g}) = \mathrm{tr}(\underset{(n-1)}{\boldsymbol{\alpha}}\,\mathbf{g}) + \frac{1}{1 + 3(2\mu + 3\lambda)\Delta\bar{\Lambda}^{(i-1)}\underset{(n-1)}{A}}\Big\{\mathrm{tr}[(\breve{\boldsymbol{\tau}} - \underset{(n-1)}{\alpha})\mathbf{g}]$$

$$- 3(2\mu + 3\lambda)\theta\,\underset{(n-1)}{\dot{\vartheta}}\,\Delta t - [\mathrm{tr}(\underset{(n-1)}{\mathbf{k}}\,\mathbf{g}) + tr(\underset{(n-1)}{\mathbf{s}}\,\mathbf{g})]\Delta t\Big\},$$

$$\boldsymbol{\tau}'^{(i)} = \underset{(n-1)}{\boldsymbol{\alpha}'} + \frac{1}{1 + 2\mu\Delta\bar{\Lambda}^{(i-1)}}\left[\breve{\boldsymbol{\tau}}' - \underset{(n-1)}{\boldsymbol{\alpha}'} - (\underset{(n-1)}{\mathbf{k}'} + \underset{(n-1)}{\mathbf{s}'})\Delta t\right].$$

5. Viscoplastic strain increment

$$\mathrm{tr}(\Delta \mathbf{e}^{p(i)}\mathbf{g}^{-1}) = 3\Delta\bar{\Lambda}^{(i-1)} \underset{(n-1)}{A}\, \mathrm{tr}[(\boldsymbol{\tau}^{(i)} - \underset{(n-1)}{\alpha})\mathbf{g}]$$
$$\mathbf{g}^{-1}\Delta \mathbf{e}'^{p(i)}\,\mathbf{g}^{-1} = \Delta\bar{\Lambda}^{(i-1)}(\boldsymbol{\tau}'^{(i)} - \underset{(n-1)}{\overset{\prime}{\alpha}}),$$

6. Viscoplastic deformation rate tensor

$$\mathbf{d}^{p(i)} = \Delta \mathbf{e}^{p(i)}/\Delta t\,, \quad \left\|\mathbf{d}^{p(i)}\right\| = (\mathbf{g}^{-1}\mathbf{d}^{p(i)}\mathbf{g}^{-1}\mathbf{d}^{p(i)})^{1/2},$$

7. Scalar multiplier $\Delta\bar{\Lambda}$(Newton's method)

$$\Delta\bar{\Lambda}^{(i)} = \Delta\bar{\Lambda}^{(i-1)} - \left[\frac{\partial\Theta(\Delta\bar{\Lambda}^{(i-1)})}{\partial\Delta\bar{\Lambda}^{(i-1)}}\right]^{-1}\Theta(\Delta\bar{\Lambda}^{(i-1)}),$$

8. Check the convergence

$$\left|\Delta\bar{\Lambda}^{(i)} - \Delta\bar{\Lambda}^{(i-1)}\right| \leq \mathrm{TOL}\ ?$$

YES: $\mathrm{tr}(\boldsymbol{\tau}\mathbf{g}) = \mathrm{tr}(\overset{\sim}{\boldsymbol{\tau}}^{(i)}\mathbf{g})$, $\boldsymbol{\tau}' = \overset{\sim}{\boldsymbol{\tau}}^{\prime(i)}$, $\mathbf{d}^p = \mathbf{d}^{p(i)}$, $\Delta\mathbf{e}^p = \Delta\mathbf{e}^{p(i)}$ go to **9**

NO: $i \leftarrow i+1$ go to **4**

9. Temperature

$$\vartheta = \underset{(n-1)}{\vartheta} + \frac{\bar{\chi}}{\underset{(n-1)}{\rho}\, c_p}\mathrm{tr}(\boldsymbol{\tau}\Delta\mathbf{e}^p) + \frac{\bar{\bar{\chi}}}{\underset{(n-1)}{\rho}\, c_p}\,\underset{(n-1)}{\Xi}\,\Delta t,$$

10. Internal state variables

$$\boldsymbol{\mu} = \underset{(n-1)}{\boldsymbol{\mu}} + \hat{\mathbf{m}}(\boldsymbol{\tau}, \underset{(n-1)}{\boldsymbol{\mu}}, \vartheta)\Delta t,$$

11. Covariant and plastic spin effects

$$\boldsymbol{\omega}^p = \bar{\eta}(\boldsymbol{\alpha}\mathbf{d}^p\mathbf{g}^{-1} - \mathbf{g}^{-1}\mathbf{d}^p\boldsymbol{\alpha}),$$
$$\mathbf{k} = \mathbf{g}^{-1}\mathbf{d}^p\boldsymbol{\tau} - \boldsymbol{\tau}\mathbf{d}^p\mathbf{g}^{-1},$$
$$\mathbf{s} = \boldsymbol{\omega}^p\mathbf{g}\boldsymbol{\tau} - \boldsymbol{\tau}\mathbf{g}\boldsymbol{\omega}^p,$$

12. Other magnitudes, which depend on the inelastic deformation (isotropic hardening-softening function, density of the material etc...)

In numerical implementations the derivative contained in the Newton's formula (Point 7) is usually calculated in an approximate way.

A mathematical proof of the convergence and stability of the presented method is an extremely difficult task. First of all, the geometrical and physical nonlinearities decide about this. Such essential features as the convergence and stability can be shown in a numerical way, solving the particular initial-boundary value problem. Such a numerical proof of the convergence and stability of that algorithm is presented in [7] for certain problem of the localized plastic deformation. The example presented below also confirms the convergence and stability of the proposed method for large number of the time increments.

4. Numerical example

The finite element [16] or finite difference [28] methods are frequently used in numerical analyses of deformation of structural elements. These methods differ in manners of space-time discretization and in approximation of functions of the evolution problem. Other numerical methods are also developed to use the possibility of effective simulation of fragmentation of structural elements [1].

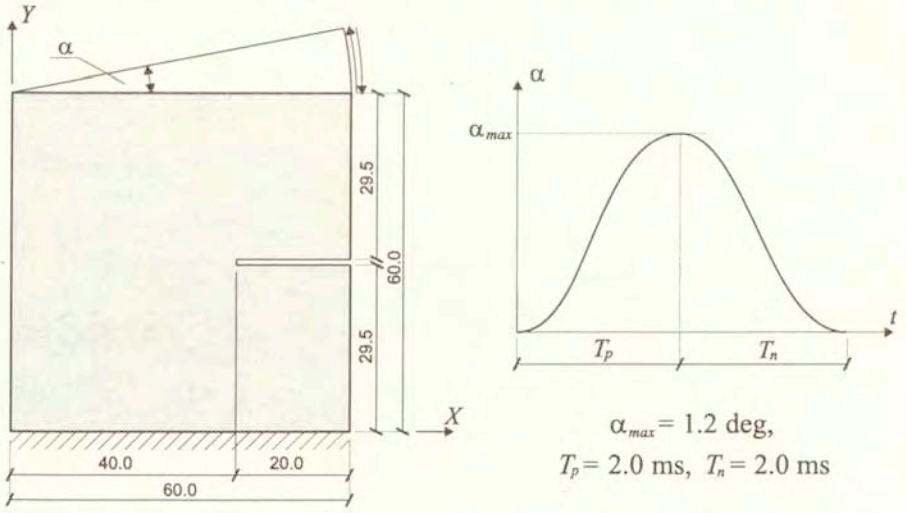

FIG. 1. Geometry and kinematic constraints of the thin steel plate with sharp notch.

The problem of fatigue crack propagation in a thin steel plate (AISI 4340) is used to illustrate the correctness of the proposed algorithm [9]. In the plate, a narrow initial notch (20 x 1 mm) is made (Fig. 1). The cyclic load realised by a rigid turn of the upper edge in relation to its left end is assumed. This load is represented by positive cycles with the amplitude $\alpha_{\max} = 1.2$ deg and with

the constant period $T = 4.0$ ms. The tensile strain time T_p and the compressive strain time T_n, are equal (Fig. 1). The number of cycles is assumed to be $N = 40$. The bottom edge of the plate ($Y = 0$) is fixed completely.

The analysis is carried out by use of the finite difference method with the explicit integration scheme with respect to time. In order to observe the local effects with great precision, a dense regular difference net (64 x 64 = 4096 nodes) is assumed. The time step assuring the stability of numerical procedure is $\Delta t = 0.1416$ μs. It leads to the total number of time increments equal to 1129943.

The isotropic work-hardening-softening function κ is postulated as [9]

$$\kappa = \hat{\kappa}(\in^p, \vartheta, \xi) \tag{4.1}$$
$$= \{\kappa_s(\vartheta) - [\kappa_s(\vartheta) - \kappa_0(\vartheta)] \exp[-\delta(\vartheta) \in^p]\} [1 - (\xi/\xi_F)^{\beta(\vartheta)}],$$

where

$$\kappa_0(\vartheta) = \kappa_0^* - \kappa_0^{**}\bar{\vartheta}, \quad \kappa_s(\vartheta) = \kappa_s^* - \kappa_s^{**}\bar{\vartheta},$$
$$\delta(\vartheta) = \delta^* - \delta^{**}\bar{\vartheta}, \quad \beta(\vartheta) = \beta^* - \beta^{**}\bar{\vartheta}, \quad \bar{\vartheta} = (\vartheta - \vartheta_0) \,/\, \vartheta_0. \tag{4.2}$$

The material parameters κ_0 and κ_s denote the yield stress and the stress at which the strain hardening saturates, respectively. The coefficients δ and β are material hardening parameters. All the material parameters are functions of temperature as in (4.2).

Thus isotropic hardening-softening effects are described by a nonlinear function depending on the equivalent plastic deformation, temperature and on the microdamage. This function determines also the local failure criterion. Let us assume that for $\xi = \xi_F$ a catastrophe takes place, that is $\kappa = \hat{\kappa}(\in^p, \vartheta, \xi)|_{\xi=\xi_F} = 0$. It means that for $\xi = \xi_F$ the material loses its carrying capacity. Such an approach is very useful to correct simulation of the fatigue crack propagation in the range of the low-cycle fatigue.

The evolution equation for the kinematic hardening parameter $\boldsymbol{\alpha}$ is assumed in the form [5]

$$L_{\mathbf{v}}\boldsymbol{\alpha} = \frac{1}{T_m} \left\langle \Phi\left(\frac{f}{\kappa} - 1\right) \right\rangle [\zeta_1(\xi, \vartheta)\mathbf{P} + \zeta_2(\xi, \vartheta)\boldsymbol{\alpha}] \tag{4.3}$$

with

$$\zeta_1(\xi, \vartheta) = \zeta_1^* - \zeta_1^{**}\bar{\vartheta}, \; \zeta_2(\xi, \vartheta) = \zeta_2^* - \zeta_2^{**}\bar{\vartheta}. \tag{4.4}$$

The kinematic hardening law (4.3) leads to the nonlinear stress-strain relation with characteristic saturation effect. The material function $\zeta_1(\xi, \vartheta)$ for $\xi = \xi_0$ and $\vartheta = \vartheta_0$ can be interpreted as an initial value of the kinematic hardening modulus

while the material function $\zeta_2(\xi, \vartheta)$ determines the character of nonlinearity of the kinematic hardening. The particular forms of the functions ζ_1 and ζ_2 have to take into account the degradation nature of the influence of the intrinsic micro-damage process on the evolution of anisotropic hardening.

The evolution equation for the porosity ξ is postulated as

$$\dot{\xi} = (\dot{\xi})_{\text{grow}} = \frac{g^*(\vartheta, \xi)}{T_m \kappa_0} \left[\tilde{I}_g - \tau_{eq}(\vartheta, \xi, \in^p) \right] \tag{4.5}$$

where [4]

$$g^*(\xi, \vartheta) = c_1(\vartheta) \frac{\xi}{1-\xi}, \quad \tilde{I}_g = b_1 \tilde{J}_1 + b_2 \sqrt{\tilde{J}_2'},$$

$$\tau_{eq}(\vartheta, \xi, \in^p) = c_2(\vartheta)(1-\xi) \ln \frac{1}{\xi} \left\{ 2\kappa_s(\vartheta) - [\kappa_s(\vartheta) - \kappa_0(\vartheta)] F(\xi_0, \xi, \vartheta) \right\},$$

$$c_1(\vartheta) = \text{const}, \quad c_2(\vartheta) = \text{const}, \tag{4.6}$$

$$F(\xi, \xi_0, \vartheta) = \left(\frac{\xi_0}{1-\xi_0} \frac{1-\xi}{\xi} \right)^{\frac{2}{3}\delta} + \left(\frac{1-\xi}{1-\xi_0} \right)^{\frac{2}{3}\delta}.$$

By $T_m \kappa_0$ we denote the dynamic viscosity of a material, $g^*(\vartheta, \xi)$ represents the void growth material function and takes into account the void interaction, $\tau_{eq}(\vartheta, \xi, \in^p)$ is the porosity, temperature and equivalent viscoplastic strain-dependent void growth threshold stress, $\tilde{I}_g$ defines the stress intensity invariant for growth, b_1 and b_2 are the material constants.

Based on the best curve fitting of the experimental results for AISI 4340 steel, the identification of the material constants has been done [9], cf. Table 1.

Table 1. Material constants for AISI 4340 steel

$\kappa_s^* = 809$ MPa	$\kappa_s^{**} = 228$ MPa	$\kappa_0^* = 598$ MPa	$\kappa_0^{**} = 168$ MPa
$\delta^* = 14.00$	$\delta^{**} = 3.94$	$\beta^* = 9.00$	$\beta^{**} = 2.53$
$\vartheta_0 = 293$ K	$\xi_F = 0.20$	$\rho_0 = 7850 \text{kg/m}^3$	$\mu = 76.92$ GPa
$\lambda = 115.38$ GPa	$\theta = 12 \cdot 10^{-6} \text{k}^{-1}$	$T_m = 2.5$ ms	$m = 1$
$\zeta_1^* = 15.00$ MPa	$\zeta_1^{**} = 4.22$ MPa	$\zeta_2^* = 69.60$ MPa	$\zeta_2^{**} = 19.60$ MPa
$c_1 = 0.202$	$c_2 = 6.7 \cdot 10^{-2}$	$b_1 = 1.0$	$b_2 = 1.30$
$\xi_0 = 6 \cdot 10^{-4}$	$\bar{\chi} = 0.85$	$\bar{\bar{\chi}} = 0.0$	$c_p = 455$ J / kg K

The distribution of the Mises stress for chosen instants during two deformation cycles is shown in Fig. 2. The results illustrate the formation of the greatest stress zones in the vicinity of the initial notch. The characteristic unsymmetrical distribution of these zones is a result of the assumed boundary conditions.

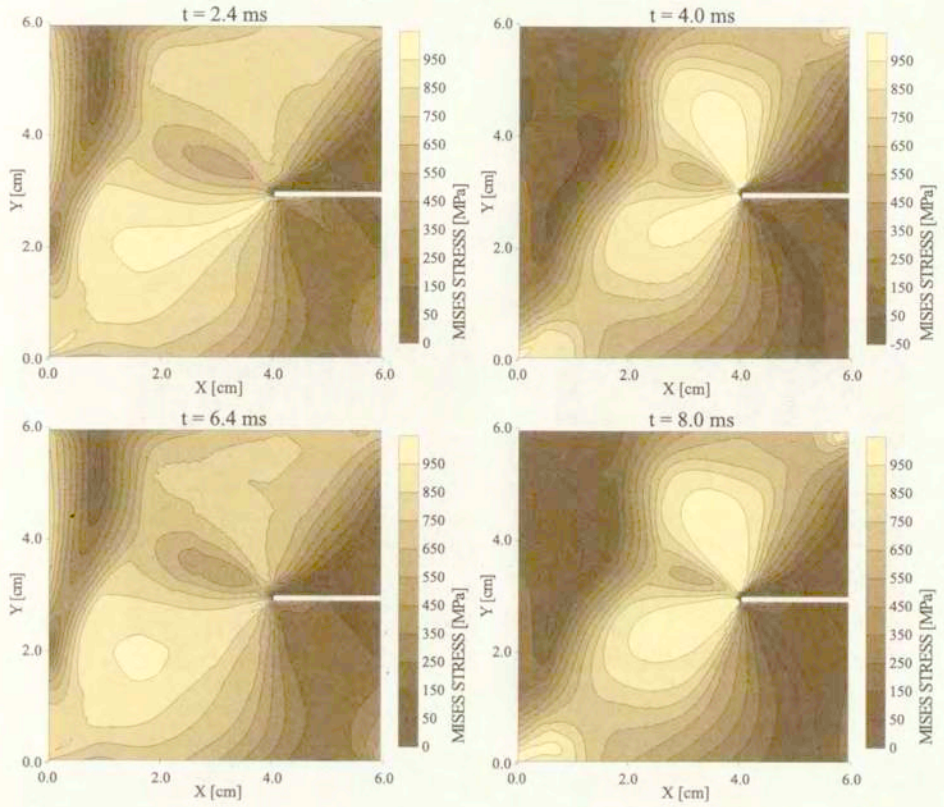

FIG. 2. Distribution of the norm of the Kirchhoff stress for chosen instants during two deformation cycles.

In Fig. 3 the evolution of the plastic equivalent deformation in the vicinity of the developed fatigue macrocrack is presented. In the initial part of the cyclic deformation process (several cycles), the plastic zone has a characteristic shape (seed of a maple). Such a form of the plastic zone has been observed experimentally. For the advanced cyclic deformation process (i.e., when the number of cycles is increased) the plastic zone is very much restricted to the vicinity of the macrocrack. The macrocrack direction is consistent with the least radius direction of the initial plastic zone. The strong concentration of plastic deformations has been seen on the front of the macrocrack.

The evolution of temperature for the considered adiabatic process is shown in Fig. 4. Zones of increased temperature correspond to the plastic zones. The maximum value of temperature is $\vartheta_{\max} = 1092$ K. The effect of such a strong heating of the material results from its mechanical properties, i.e. the high strength steel ($R_m = 1400$ MPa).

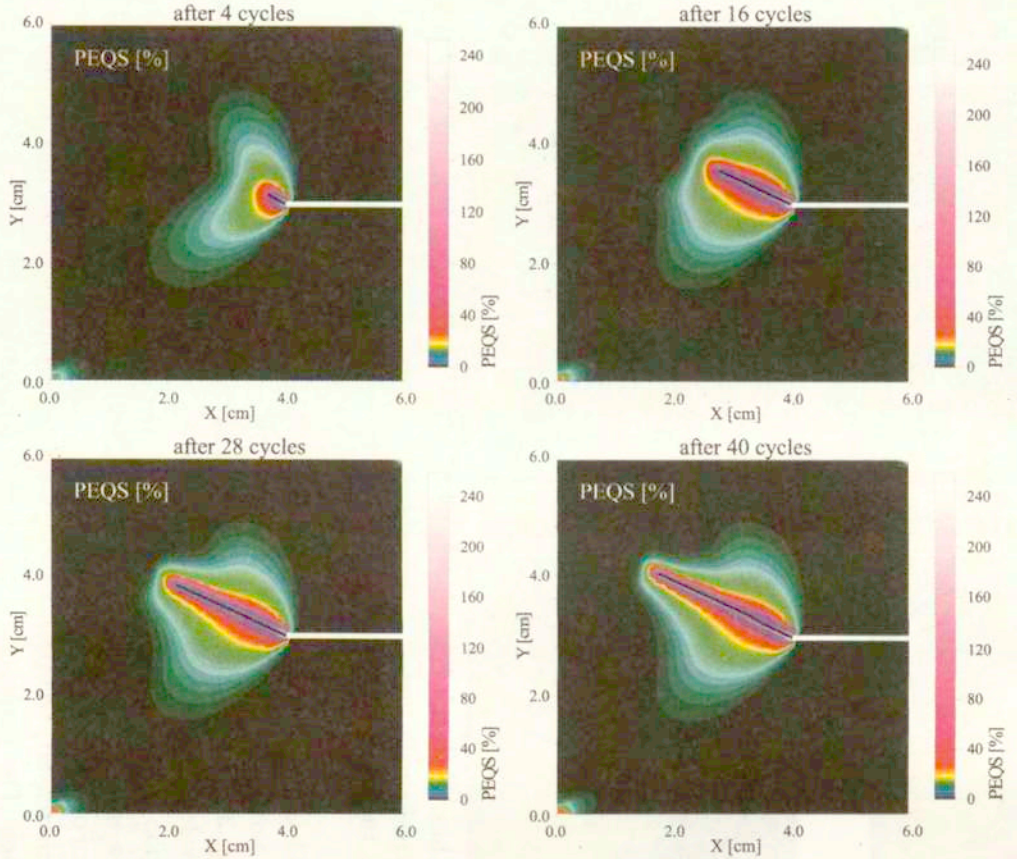

FIG. 3. Evolution of the equivalent plastic deformation in the vicinity of the developed fatigue damage.

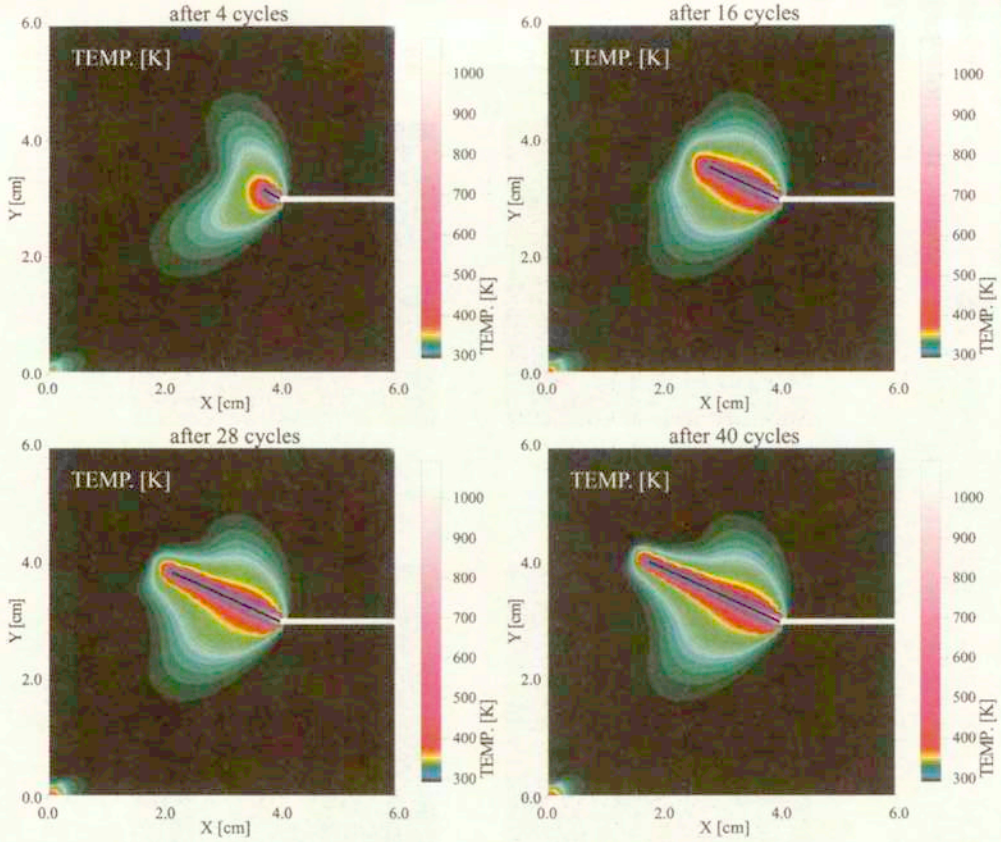

FIG. 4. Evolution of temperature in the vicinity of the developed fatigue damage.

In Fig. 5 the evolution of microdamage is presented. The domain of microdamage is limited to the vicinity of the macrocrack. This effect is a result of the strong concentration of the microdamage process on the front of the macrocrack. The complex evolution of the plastic rotation is shown in Fig. 6. In the domain lying above the macrocrack the plastic rotation has negative value, i.e. the rotation in the left direction in relation to the assumed coordinate system, while in the domain lying below the macrocrack it has a positive value. It is noteworthy that the border between these two domains is consistent with the macrocrack direction.

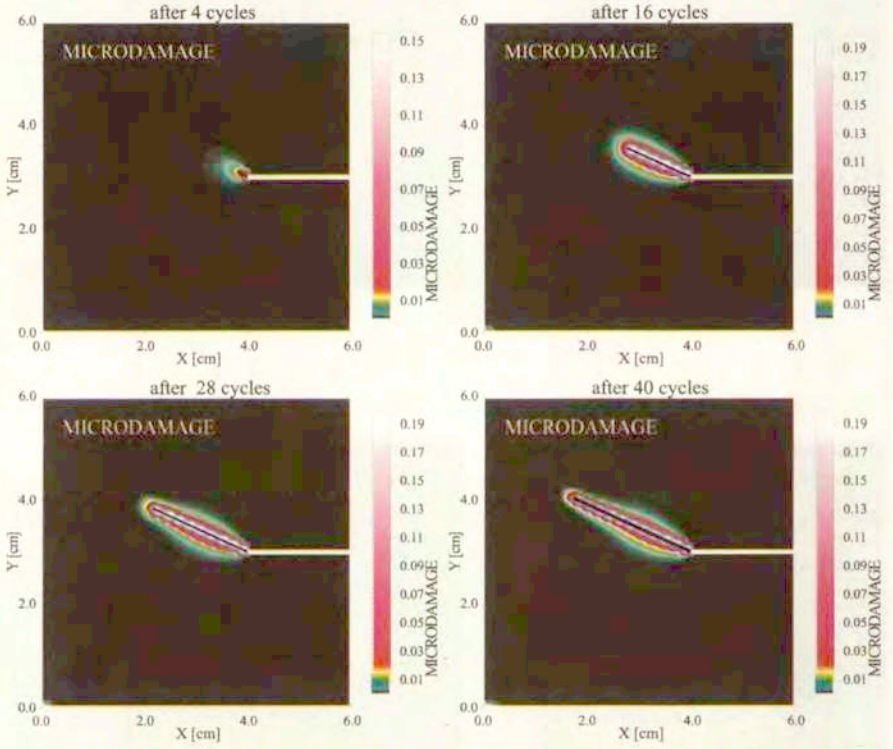

FIG. 5. Evolution of the microdamage in the vicinity of the developed fatigue damage.

The analyzed fatigue damage process at high temperature is very complex. The experimental observations performed in [30] show that the decrease in fatigue life is associated with a change in the fracture mode from transgranular to intergranular cracking. The microdamage kinetics interacts with thermal and load changes to make failure of solids a highly rate, temperature and history-dependent, nonlinear process. The incorporation of these effects in the presented constitutive model required considering the general constitutive structure with internal state variables for polycrystalline solids.

The constitutive description of internal micro-damage process required a special care [4]. This process was treated as a sequence of nucleation, growth and coalescence of microcracks. Evolution equations based on the concept of threshold stresses for nucleation and growth processes are assumed. It made possible the correct description of damage fatigue accumulation.

It is noteworthy that the presented description of the thermodynamical process of inelastic flow is internally regularized [19], in this case the time of mechanical relaxation is a regularization parameter. From a computational standpoint this property is of a very important significance, because it assures the unique numerical solution.

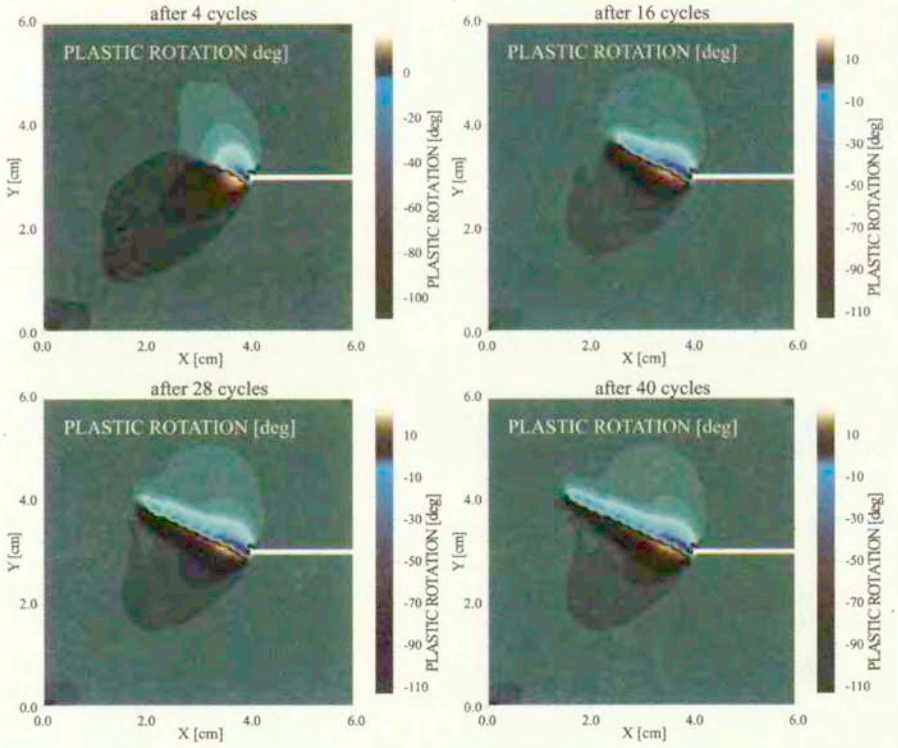

FIG. 6. Evolution of the plastic rotation in the vicinity of the developed fatigue damage.

5. Final comments

The performed numerical simulations of the dynamic, cyclic loading process have proven the usefulness of the proposed numerical integration algorithm in the investigation of localized fatigue fracture phenomena. The material objec-

tivity with respect to the total motion (translation, rotation and strain) of a material element is preserved. The way in which the incremental form of the plastic flow rule is obtained and the way of determining the flow stresses decide on the originality of the algorithm and differentiate it from the return mapping algorithms.

The proposed algorithm is very effective and it can be used to the numerical analysis of large deformations and fracture in metal structural elements under monotonic loadings too.

Acknowledgement

The paper has been prepared within the research programme sponsored by the Committee of Scientific Research under Grant 7T07A00616.

References

1. T. BELYTSCHKO and M. TABBARA, *Dynamic fracture using element-free Galerkin methods*, International Journal for Numerical Methods in Engineering, **39**, 923–938, 1996.
2. Y. F. DAFALIAS, *Corotational rates for kinematic hardening at large plastic deformations*, J. Appl. Mech., **50**, 561–565, 1983.
3. W. DORNOWSKI, *A constitutive model for a cyclically loaded material with microdamages*, Bull. MUT, **2**, 95–117, 1998.
4. W. DORNOWSKI, *Influence of finite deformations on the growth mechanism of microvoids contained in structural metals*, Arch. Mech., **51**, 71–86, 1999.
5. W. DORNOWSKI, *Numerical simulations of plastic flow processes under cyclic dynamic loadings*, MUT 2598/99, Warsaw 1999.
6. W. DORNOWSKI and P. PERZYNA, *Constitutive modeling of inelastic solids for plastic flow process under cyclic dynamic loadings*, Journal of Engineering Materials and Technology, ASME, **121**, 210–220, 1999.
7. W. DORNOWSKI and P. PERZYNA, *Localization phenomena in thermo-viscoplastic flow processes under cyclic dynamic loadings*, Computer Assisted Mechanics and Engineering Sciences, **7**, 117–160, 2000.
8. W. DORNOWSKI and P. PERZYNA, *Numerical simulations of thermo-viscoplastic flow processes under cyclic dynamic loadings*, In: Proc. Euromech Colloquium 383, Inelastic Analysis of Structures under Variable Loads: Theory and Engineering Applications D. WEICHERT and G. MAIER [Eds.], Kluwer Academic Publishers, 69–94, 2000.
9. W. DORNOWSKI and P. PERZYNA, *Localized fracture phenomena in thermo-viscoplastic flow processes under cyclic dynamic loadings*, Acta Mechanica, **30**, 1–23, 2001.
10. M. DUSZEK and P. PERZYNA, *Plasticity of damage solids and shear band localization*, Ingenieur-Archiv., **58**, 380–392, 1988.
11. M. K. DUSZEK and P. PERZYNA, *The localization of plastic deformation in thermoplastic solids*, Int. J. Solids Structures, **27**, 11, 1419–1443, 1991.

12. M. K. DUSZEK-PERZYNA and P. PERZYNA, *Adiabatic shear band localization in elastic-plastic single crystals*, Int. J. Solids Structures, **30**, 61–89, 1993.

13. A. E. GREEN and W. ZERNA, *Theoretical elasticity*, Second Edition, Clarendon Press, Oxford 1960.

14. R. HILL, *Aspects of invariance in Solid Mechanics*, Advances in Applied Mechanics, **18**, 1–75, 1978.

15. T. J. R. HUGHES and J. WINGET, *Finite rotation effects in numerical integration of rate constitutive equations arising in large-deformation analysis*, International Journal for Numerical Methods in Engineering, **15**, 9, 1413-1418, 1980.

16. M. KLEIBER and C. WOŹNIAK, *Nonlinear mechanics of structures*, PWN, Warsaw, Kluwer Academic Publishers, Dordrecht/Boston/London, 1991.

17. R. D. KRIEG and S. W. KEY, *Implementation of a time dependent plasticity theory into structural computer programs*, Constitutive Equations in Viscoplasticity, Computational and Engineering Aspects, J.A. STRICKLIN and K.J. SACZLSKI [Eds.], AMD-20, ASME, New York 1976.

18. R. D. KRIEG and D. B. KRIEG, *Accuracies of numerical solution methods for the elastic-perfectly plastic model*, Journal of Pressure Vessel Technology, ASME, **99**, 1977.

19. T. ĆODYGOWSKI and P. PERZYNA, *Localized fracture in inelastic polycrystalline solids under dynamic loading processes*, Int. J. Damage Mechanics, **6**, 364-407, 1997.

20. J. E. MARSDEN and T. J. R. HUGHES, *Mathematical Foundations of Elasticity*, Prentice-Hall, Englewood Cliffs, NY 1983.

21. A. NEEDLEMAN and V. TVERGAARD, *Finite element analysis of localization plasticity*, [in:] Finite Elements, Vol V: Special problems in solid mechanics, J. T. ODEN and G. F. CAREY [Eds.], Prentice-Hall, Englewood Cliffs, New Jersey 1984.

22. M. ORTIZ and J. C. SIMO, *An analysis of a new class of integration algorithms for elasto-plastic constitutive relations*, International Journal for Numerical Methods in Engineering, **23**, 353–366, 1986.

23. P. PERZYNA, *The constitutive equations for rate sensitive plastic materials*, Q. Appl. Math., **20**, 321–332, 1963.

24. P. PERZYNA, *Theory of viscoplasticity*, PWN, Warsaw 1966.

25. P. PERZYNA, *Thermodynamics of inelastic materials*, PWN, Warsaw 1978.

26. P. PINSKY, M. ORTIZ and K. S. PISTER, *Numerical integration of rate constitutive equations in finite deformation analysis*, Computer Methods in Applied Mechanics and Engineering, **40**, 137–158, 1983.

27. J. R. RICE and D. M. TRACEY, *Computational fracture mechanics*, In Proceedings of the Symposium on Numerical Methods in Structural Mechanics, S. J. FENVES [Ed.], Academic Press, Urbana Illinois 1973.

28. R. D. RICHTMYER and K. W. MORTON, *Difference methods for initial-value problems*, Interscience Publishers, 2^{nd} edition, New York 1967.

29. R. RUBINSTEIN and S. N. ATLURI, *Objectivity of incremental constitutive relations over finite time step in computational finite deformation analyses*, Computer Methods in Applied Mechanics and Engineering, **36**, 1983.

30. D. SIDEY and L. F. COFFIN, *Low-cycle fatigue damage mechanisms at high temperature*, Fatigue Mechanisms, Proceedings of an ASTM-NBS-NSF symposium, Kansas City, Mo., May 1978, J. T. FONG [Ed.], ASTM STP 675. American Society for Testing and Materials, 528–568, 1979.

31. J. C. SIMO and M. ORTIZ, *A unified approach to finite deformation elastoplasticity based on the use of hyperelastic constitutive equations*, Computer Methods in Applied Mechanics and Engineering, **49**, 221-245, 1985.

32. J. C. SIMO, *Algorithms for static and dynamic multiplicative plasticity that preserve the classical return mapping schemes of the infinitesimal theory*, Computer Methods in Applied Mechanics and Engineering, **99**, 61-112, 1992.

33. M. L. WILKINS, *Calculation of elastic-plastic flow*, In Methods of Computational Physics 3, Editors B. Alder *et. al.*, Academic Press, New York 1964.

Received May 28, 2002; revised version September 19, 2002.